

# Massive stars in the Sagittarius Dwarf Irregular Galaxy <sup>★</sup>

Miriam Garcia<sup>1</sup> <sup>†</sup>

<sup>1</sup>Centro de Astrobiología (CSIC-INTA). Crtra. de Torrejón a Ajalvir km 4. 28850 Torrejón de Ardoz (Madrid), Spain

Accepted XXX. Received YYY; in original form ZZZ

## ABSTRACT

Low metallicity massive stars hold the key to interpret numerous processes in the past Universe including re-ionization, starburst galaxies, high-redshift supernovae and  $\gamma$ -ray bursts. The Sagittarius Dwarf Irregular Galaxy (SagDIG,  $12+\log(\text{O}/\text{H})=7.37$ ) represents an important landmark in the quest for analogues accessible with 10-m class telescopes. This paper presents low-resolution spectroscopy executed with the Gran Telescopio Canarias that confirms that SagDIG hosts massive stars. The observations unveiled three OBA-type stars and one red supergiant candidate. Pending confirmation from high-resolution follow-up studies, these could be the most metal-poor massive stars of the Local Group.

**Key words:** Stars: massive – Stars: early-type – Galaxies: individual: SagDIG – Galaxies: stellar content

## 1 INTRODUCTION

Understanding the evolution of very metal-poor massive stars is key to interpret star formation and feedback at previous Cosmic epochs, and a necessary step towards the physics of the first stars of the Universe. This has stimulated an enthusiastic effort to discover resolved massive stars in environments of decreasing metal content, mostly dwarf irregular galaxies of the Local Group.

The Small Magellanic Cloud (SMC) is the current standard for the low- $Z$  regime, but metal-poorer massive stars are now at reach with multi-object spectrographs at 8–10m telescopes. First quantitative analyses were directed to the IC 1613, NGC 3109 and WLM galaxies (Bresolin et al. 2007; Herrero et al. 2010; Trammer et al. 2011) with encouragingly low  $1/7\text{O}_{\odot}$  oxygen abundances, but subsequent studies indicate that their iron content is SMC-like ( $\sim 1/5\text{Fe}_{\odot}$ ) instead (Garcia et al. 2014; Hosek et al. 2014; Bouret et al. 2015). Following efforts were directed to Sextans A (Camacho et al. 2016) with both  $1/10\text{Fe}_{\odot}$  and  $1/10\text{O}_{\odot}$  (Kaufer et al. 2004). However, this value is still far from the  $\sim 1/30Z_{\odot}$  average metallicity of the Universe at the peak of star formation history and from measurements of the intergalactic medium at higher redshifts (Madau & Dickinson 2014).

The Sagittarius Dwarf Irregular Galaxy (*aka* Sgr dIG, ESO 594-4, UKS 1927-17.7; SagDIG from now on) makes a promising environment to find very metal-poor, resolved massive stars. Its intermediate-age population stands out as one of the most Fe-poor among the Local Group galaxies that sustain star formation (e.g. McConnachie 2012), with values inferred from the location

of the red giant branch (RGB) that range from  $[\text{Fe}/\text{H}]=-2.0$  to  $-2.45$  (Beccari et al. 2014; Karachentsev et al. 1999). Regarding the youngest populations, the oxygen abundance determined from the only confirmed H II region SagDIG-HII#3 (Strobel et al. 1991) is also remarkably low  $12+\log(\text{O}/\text{H})=7.37^{+0.13}_{-0.11}$  (Saviane et al. 2002). Scaled by the Solar photospheric abundance (Asplund et al. 2009), this value is equivalent to  $1/21\text{O}_{\odot}$ .

While SagDIG is considered one of the extremely metal-poor galaxies of the Local Universe, rivaling I Zw18 (Filho et al. 2015), it has never been explored for massive stars. This paper presents the first spectroscopic observations of young massive stars in the galaxy. Section 2 describes the observations and data reduction. Target identification, spectral types and membership are assessed in Section 3. The discovered red supergiant candidate is discussed in the context of the Local Group in Section 4. Finally, summary and some prospects for future work are provided in Section 5.

## 2 DATA AND REDUCTION

The observations were executed with the OSIRIS spectrograph at the 10.4-m Gran Telescopio Canarias (GTC), programme GTC67-13A (PI M. Garcia). The 1.2 arcsec slit and R2000B VPH were used to achieve resolution  $R \sim 1000$  at  $\sim 4000\text{--}5500\text{\AA}$ . The slit was aligned on targets SD-1 and SD-7 to cross the galaxy (Fig. 1) and enclose several UV-bright sources. A total of 2 hours of grey sky, 1.2 arcsec seeing exposure time were devoted to the slit.

The data were reduced following standard IRAF<sup>1</sup> procedures adapted for the team’s OSIRIS runs (Garcia & Herrero 2013).

<sup>★</sup> Based on observations made with the Gran Telescopio Canarias (GTC), installed in the Spanish Observatorio del Roque de los Muchachos of the Instituto de Astrofísica de Canarias, on the island of La Palma.

<sup>†</sup> E-mail: mgg@cab.inta-csic.es

<sup>1</sup> IRAF is distributed by the National Optical Astronomy Observatory, operated by the Association of Universities for Research in Astronomy (AURA) under agreement with the National Science Foundation.

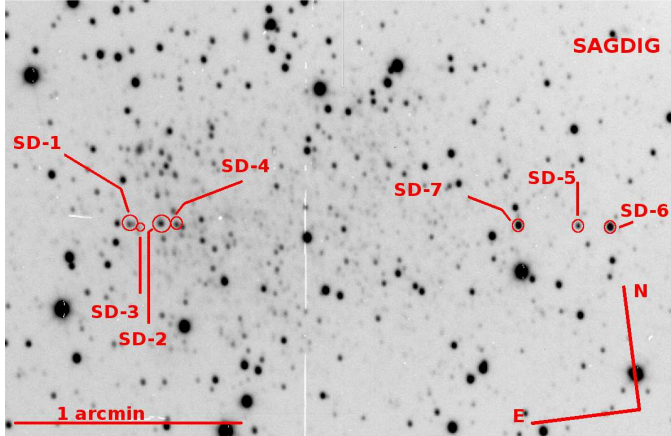


**Figure 1.** SagDIG: GTC–OSIRIS acquisition image (1.2 arcsec seeing, filter–free), and programme stars.

The spectra were flux–calibrated against the flux standard GD190, achieving about 5 per cent accuracy for  $\lambda > 4250\text{\AA}$ . Finally, the spectra were set to the heliocentric frame and corrected by radial velocity. The latter were calculated from the Doppler shift measured at the core of the Balmer lines. The reduced spectra are shown in Figs. 2–3.

The programme faced the challenges related to observations of faint, distant stars: contamination by nearby sources and small number of counts over the background level. For instance the spectrum of SD-1, with  $V \sim 20.2$ , registered a factor  $\sim 2.5$  less counts than the extracted sky spectrum. The resulting signal to noise ratio (SNR) is consequently poor even after careful sky subtraction and some Solar features remained. These shortcomings discourage future optical range spectroscopic observations of targets fainter than  $V=20$  mag in grey time.

Targets SD-1 to 4 are found in an area of extended continuum emission (detected in Far–Ultraviolet imaging as well, e.g. Momany et al. 2014) that may contaminate the extracted spectra. In order to minimize blends, the sources were extracted discarding the wings of the spatial distribution of photons in the 2-D images.

### 3 SOURCE IDENTIFICATION, SPECTRAL CLASSIFICATION AND MEMBERSHIP

SagDIG is projected close to the Galactic Centre and the line of sight is severely contaminated with Milky Way stars. Hence, ensuring that the programme targets belong to the galaxy was an issue. This section discusses jointly target identification, spectral classification, membership, and their consistency. The location of the programme stars in the colour–magnitude diagram (CMD) is evaluated as a final check.

The programme targets were identified in the Beccari et al. (2014, hereafter B14) and Momany et al. (2014, M14) catalogues by comparing the GTC acquisition images against HST–ACS archival observations (GO-9820 P.I. Y. Momany). Identification numbers and photometry are listed in Table 1.

The spectral classification of blue stars, whose most prominent spectral feature is the Balmer series, was carried out following classical criteria (see e.g. Garcia & Herrero 2013). Their spectra are shown in Fig. 2. The rest of the sample (Fig. 3) was classified after Dorda (2016)’s scheme for cool stars (G–types and later)

in the LMC and the SMC, and the spectral classification atlas by Gray (2000)<sup>2</sup>. They were also compared against SMC and MW standards.

Membership of the programme stars with counterpart in M14’s catalogue, that registered relative shifts from multi-epoch HST visits, was ensured by the lack of proper motions. In addition, the estimated absolute magnitudes were compared against the calibrated values for the spectral types assigned in this work. The consistency of the stellar radial velocities and SagDIG’s systemic velocity ( $-78.5 \text{ km s}^{-1}$ , McConnachie 2012) was not determinant because of the low spectral resolution of these observations ( $\sim 300 \text{ km s}^{-1}$ , hence typical  $v_{\text{rad}}$  uncertainties of  $\sim 100 \text{ km s}^{-1}$ ).

The following subsections provide more details on the targets that were positively identified as SagDIG massive stars.

#### 3.1 SD-1

The HST–ACS images reveal that SD-1 is the blend of two stars  $\sim 1.1$  arcsec apart, SD-1-blue (M14-33466; B14-8903,  $V=20.190$ ) and SD-1-red (B14-8909,  $V=21.774$ ). SD-1 will be identified with the brightest star of the blend, SD-1-blue, from now on.

The Balmer series is clearly detected in its spectrum (Fig. 2), and the comparison against the sky spectrum confirms that the stellar component dominates  $H\gamma$  and  $H\beta$ . The data also display  $\text{He I } 4026\text{\AA}$ ,  $\text{He I } 4387\text{\AA}$  and  $\text{He I } 4471\text{\AA}$ , but the detection of  $\text{He II}$  lines is unclear.  $\text{He II } 4541\text{\AA}$  is absent and the  $\text{He II } 4200\text{\AA}$  and  $\text{He II } 5411\text{\AA}$  absorptions overlap with sky features.

The exception is  $\text{He II } 4686\text{\AA}$ , detected in emission. Its width together with the absence of  $\text{H I}$  and  $\text{He I}$  emission lines renders a nebular origin unlikely, and the comparison against the subtracted sky spectrum discards the feature as an artefact. The  $\text{He II } 4686\text{\AA}$  emission could be consistent with a late–O type, with the rest of  $\text{He II}$  lines too weak for detection at the SNR of the spectrum. The non–detection of  $\text{Mg II } 4481\text{\AA}$  and  $\text{Si III } 4552\text{\AA}$  supports the late–O classification, although it could also be caused by the low metallicity of the star.

The spectrum of SD-1 is reminiscent of star C1\_31 in NGC 55 (Castro et al. 2008). C1\_31 is mostly featureless except for the Balmer lines and a prominent broad  $\text{He II } 4686\text{\AA}$  emission, with  $\text{He I } 4471\text{\AA}$  clearly seen but no  $\text{He II } 4541\text{\AA}$ . It was classified as early–O supergiant. Similarly, SD-1 is classified as late–O I, with the  $\text{He II } 4686\text{\AA}$  emission and narrow Balmer lines supporting the supergiant luminosity class. The estimated absolute magnitude  $M_V = -6.1$  agrees with the calibrated value for late–O supergiants (Massey 1998).

#### 3.2 SD-2

SD-2 is the blend of M14-31722 ( $F606W=20.278$ ) and M14-31570 ( $F606W=21.839$ ), 0.7 arcsec apart and unresolved. SD-2 is identified with the brightest source M14-31722.

Its spectrum shows the Balmer series,  $\text{He I } 4471\text{\AA}$ ,  $\text{He I } 4387\text{\AA}$  and  $\text{He I } 4922\text{\AA}$  (Fig. 2). There may be some  $\text{Mg II } 4481\text{\AA}$ , but no lines of  $\text{Si III}$ ,  $\text{Si IV}$  or  $\text{He II}$ . The calibrated stellar flux corresponds to a colder object than SD-1. Since the width of the Balmer lines is similar to SD-1, and the strength of the  $\text{He I}$  lines is almost at noise level, SD-2 is classified as a BA-supergiant. The estimated absolute magnitude  $M_V = -5.1$  is consistent with a blue supergiant located at SagDIG.

<sup>2</sup> <https://ned.ipac.caltech.edu/level5/Gray/frames.html>

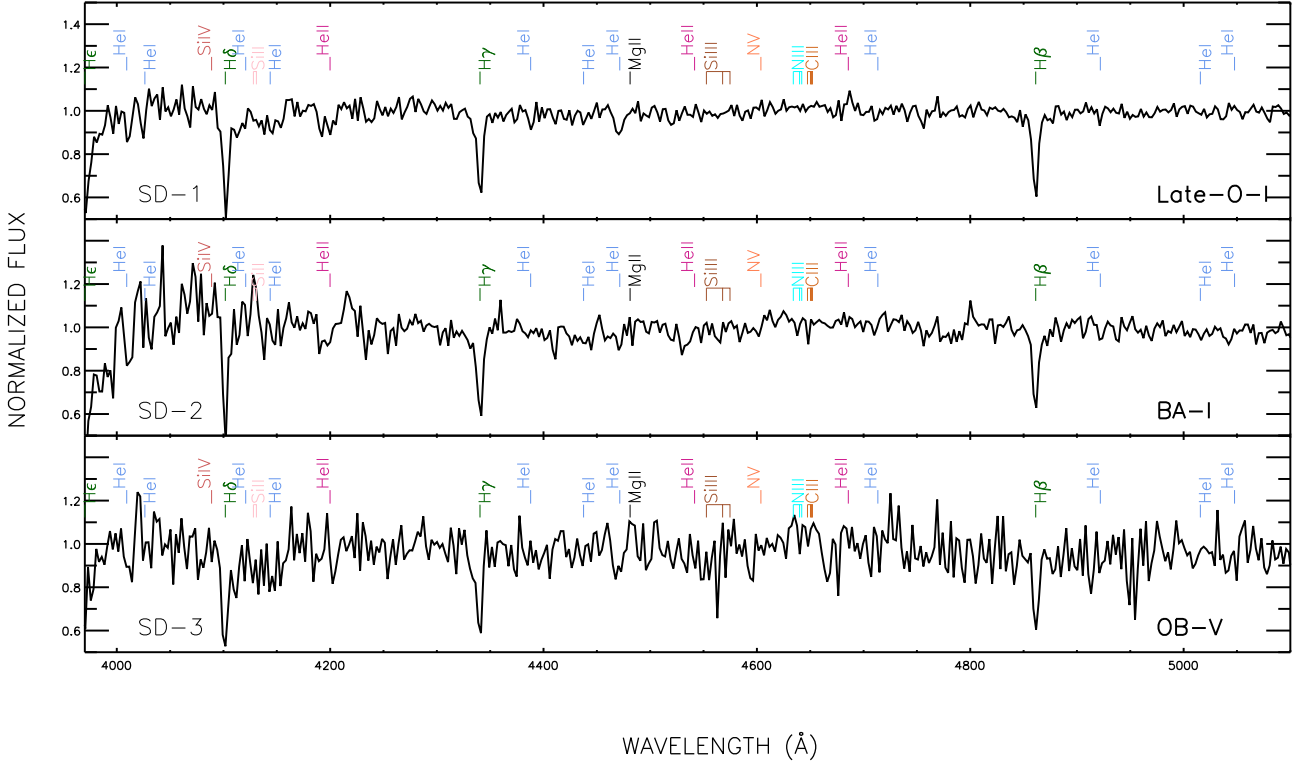


**Figure 2.** GTC-OSIRIS spectra of blue massive stars in SagDIG. The data have been rebinned to 3 pixels for clarity, and corrected by heliocentric and radial velocity. The three spectra show a clear Balmer series.

**Table 1.** Observed stars: spectral types (SpT) from this work, radial velocities ( $v_{\text{rad}}$ ) used in Figs. 2–3, and cross-identification numbers and photometry from M14 and B14.  $M_V$  was computed from apparent magnitudes, distance modulus (SagDIG stars: DM=25.10 [Momany et al. \(2005\)](#); foreground stars: DM=14.50), and [Cox \(2000\)](#)'s intrinsic colors to estimate  $E(V-I)$  and correct from extinction. The last column flags SagDIG membership.

ID	SpT	$v_{\text{rad}}$ [km s <sup>-1</sup> ]	M14 ID	F475W	F606W	F814W	B14 ID	$V$	$I$	$E(V-I)$	$M_V$	Memb.
SD-1	Late-O I	-65	33466	20.189	20.125	20.024	8903	20.190	20.154	0.51	-6.1	yes
SD-2	BA I	-55	31722	20.355	20.278	20.120	‡	20.38	20.24	0.12	-5.1	yes
SD-3	OB V	-95	32939	21.408	21.480	21.515	8822	21.442	21.585	0.28	-4.3	yes
SD-4	G0-2 I	-100	30481	21.558	20.503	19.394	8805	20.731	19.473	0.42	-5.3	yes
SD-5	G4 III	-90	3019	20.887	20.055	19.144	‡	20.38	19.23	0.26	5.3	fg
SD-6	G5 V	-70	†		18.59	17.82	7783	18.875	17.912	0.07	4.2	fg
SD-7	K4 V	-50	†		18.76	17.74	8017	19.124	17.819	0.42	3.7	fg

(†) Star without M14-counterpart. F606W and F814W magnitudes estimated from B14's  $V$ - and  $I$ -magnitudes, using [Rejkuba et al. \(2005\)](#)'s transformations.

(‡) Star without B14-counterpart.  $V$ -magnitudes estimated from M14, using [Rejkuba et al. \(2005\)](#)'s transformations.

### 3.3 SD-3

Target SD-3 is faint and off-slit, resulting in extremely low spectral SNR. The sky contribution amounts to 83 per cent of the total flux at blue wavelengths, increasing to 91 per cent at 4800Å.

SD-3 overlaps with the red component of the SD-1 blend. However, there is a shift between SD-3's strongest features and the same lines in SD-1 reflecting the different radial velocities of the two stars and confirming that the lines genuinely belong to SD-3.

The spectrum of SD-3 (Fig. 2) exhibits the Balmer series and He I 4471Å. The He II lines, but also Si III 4552Å and Mg II 4481Å, are absent suggesting late-O or early-B spectral type. The spectrum lacks any He II 4686Å, but contamination by SD-1-red begins to be significant in this region. The wings of H $\gamma$  are dominated by

the stellar component, and the profile is wider than SD-1's, suggesting class III or V. Since the absolute magnitude agrees with [Massey \(1998\)](#)'s calibration for O9–B0 V ( $M_V = -4.4$  to  $-3.8$ ), SD-3 is classified as an OB-dwarf.

### 3.4 SD-4

SD-4 (M14-30481, F606W=20.503) is contaminated by a nearby red star with similar magnitude (M14-30025, F606W=20.360). According to their proper motions, both belong to SagDIG.

Luminosity class was constrained in the first place, following [Dorda \(2016\)](#). Because the 5167Å component is the strongest of the magnesium triplet Mg I 5167, 5172, 5184Å, SD-4 was classified

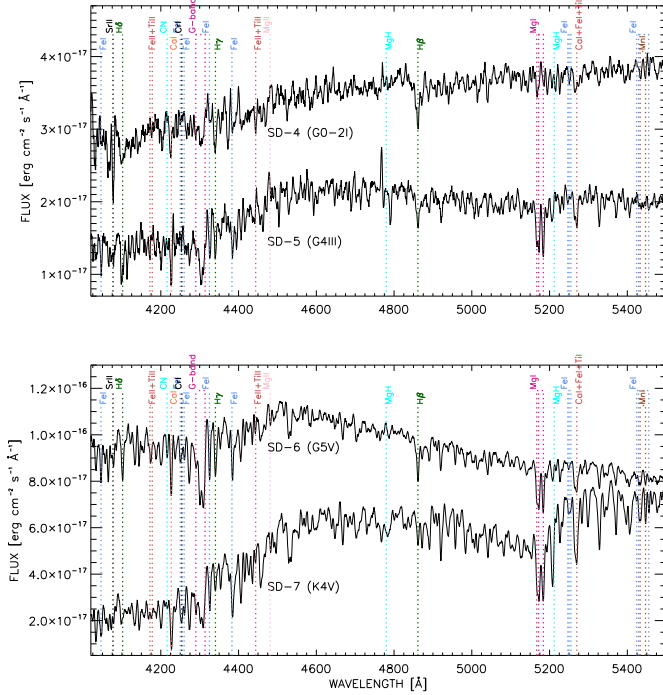


**Figure 3.** Red programme stars. The flux-calibrated spectra were smoothed to 5 points, and corrected by heliocentric and radial velocity. In both panels the upper spectrum has been shifted by a constant for clarity (SD-4:  $1.5E-17$  erg cm $^{-2}$  s $^{-1}$  Å $^{-1}$ , SD-6:  $3E-17$  erg cm $^{-2}$  s $^{-1}$  Å $^{-1}$ ).

a supergiant. The relative strength of Fe I 5247, 5250, 5255 Å vs Ca I + Fe I + Ti I 5270 Å, and Mn I 5433 Å vs Mn I 5447 Å support this luminosity class.

The presence of the G-band and its relative strength compared to  $H\gamma$  and Ca I 4227 Å suggests that the spectral type is slightly later than G0. The relative strength of Fe I 4325 Å compared to both  $H\gamma$  and Fe I 4383 Å, on the other hand, suggests spectral type G0 or earlier. A G0–2 I type is finally assigned.

It is noted that the estimated absolute magnitude  $M_V = -5.3$  is slightly fainter than the calibrated  $M_V = -6.4$  G0 I. Nevertheless, SD-4's membership to SagDIG is supported by the lack of detection of proper motions by M14. Since red supergiants (RSG) stars may experience spectral variability (see Sect. 4), SD-4 is proposed as a RSG-candidate in SagDIG.

### 3.5 Target stars in the colour-magnitude diagram

The location of the target stars in the CMD is consistent with the spectral types assigned in this work (Fig. 4). The three OBA stars are found in the upper part of the blue plume. The red stars SD-5, SD-6 and SD-7 are enclosed in the vertical sequence of Galactic foreground contamination. SD-4, on the other hand, is above the tip of the RGB consistently with the star being a red-supergiant.

The loci of the youngest stars in the CMD is also consistent with the theoretical isochrones ( $Z=0.001$  or  $\sim 1/15 Z_\odot$  Marigo et al. 2017) but require a larger correction than the reported  $E(B-V)_{fg} = 0.12$  foreground extinction (e.g. Momany et al. 2005). Internal reddening can indeed be expected, since SD-1 to 4 are located in a concentration of neutral hydrogen (Young & Lo 1997, also B14). The  $E(B-V) \approx 0.22$  colour excess calculated from

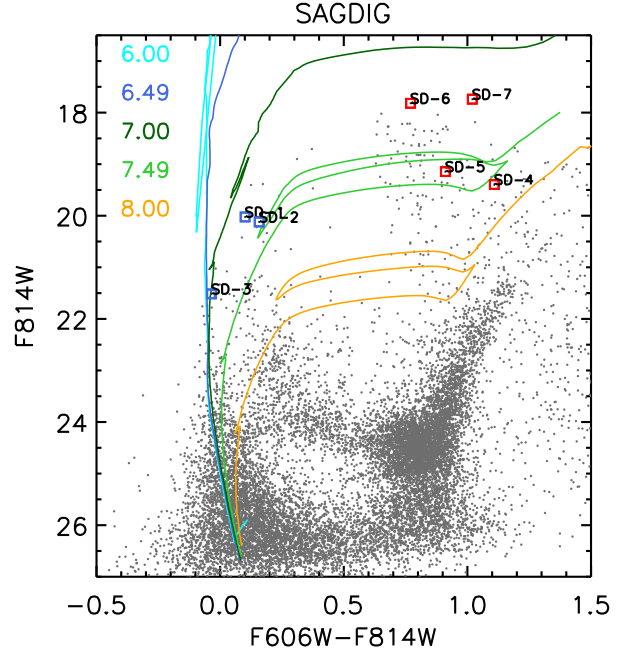


**Figure 4.** SagDIG's colour-magnitude diagram built from M14's catalogue (grey dots). Marigo et al. (2017)'s isochrones for  $Z=0.001$  ( $\sim 1/15 Z_\odot$ ) are included for comparison, with colour coding  $\log(\text{ageyrs})=6.0, 6.49, 7.0, 7.49, 8.0$ . Younger isochrones are not included because they overlap at  $F606W-F814W \sim 0$  in the  $F814W=20-22$  range. The isochrones were shifted by SagDIG distance modulus  $(m-M)_0=25.10$  and reddened by the equivalent to  $E(B-V)=0.22$  ( $A_{F606W}=0.646$ ,  $A_{F814W}=0.410$ , after Sirianni et al. (2005)).

the Balmer decrement of SagDIG-HII#3 was adopted (Lee et al. 2003; Tang et al. 2016).

SD-3 is located at the main sequence where isochrones of  $\log(\text{ageyrs})=4.5-7.0$  overlap, in accordance with its OB V spectral type. SD-2 is found between the  $\log(\text{ageyrs})=7.0$  and 7.49 isochrones, as expected considering that BA-supergiants have evolved off the main sequence and are slightly older than O-stars. The location of SD-4 is consistent with a RSG with similar age  $\log(\text{ageyrs})=7.49$ .

SD-1 is found between the  $\log(\text{ageyrs})=7.0-7.49$  isochrones, however, it is more reddened than the other programme stars. If its  $E(B-V)=0.38$  spectroscopic colour excess is taken at face value, the isochrones would need an additional shift of  $\Delta(F606W-F814W) \sim 0.2$  mag and  $\Delta F814W \sim 0.3$  mag to account for the increased extinction. This would bring SD-1 close to the  $\log(\text{ageyrs})=6.49$  isochrone (3 Myr), that better agrees with the expected age of an O-type supergiant.

The unknown amount of internal reddening in SagDIG hinders the interpretation of the CMD (SD-1,2,3 would be mistaken as intermediate-mass stars if  $E(B-V)_{fg}$  was used) and may hide a significant population of young and massive stars. Extinction can explain the paucity of stars in the upper blue plume, which is at odds with the extended emission of the galaxy in the UV. These results may be considered a reminder that the total galactic stellar content may be underestimated from the luminosity function, and advises against selecting massive star candidates from their location in classical CMDs only.

#### 4 THE MOST METAL-POOR RSG TO DATE

Red supergiants are He–burning descendants of  $M_{\text{ini}} \lesssim 30 M_{\odot}$  stars and the coolest stage in the life-cycle of massive stars. They are gathering increased interest because some RSGs ( $9 < M_{\text{ini}} < 16.5$ – $23 M_{\odot}$ ) are the alleged progenitors of type-IIP supernovae (Groh et al. 2013). Besides, they are proving reliable metallicity probes optimally reached by current, powerful IR spectrographs: Keck–NIRSPEC, GTC–EMIR or VLT–KMOS (e.g. Davies et al. 2009; Gazak et al. 2015).

Red supergiants are classically associated with M-types, but the average spectral type shifts towards earlier types in metal-poorer galaxies (Elias et al. 1985; Levesque & Massey 2012). This trend is beyond a classification bias produced by the weakening of TiO bands when metallicity decreases, and it is believed to reflect the fact that the Hayashi limit shifts towards higher effective temperatures with decreasing metallicity (see discussion by Elias et al. 1985). For this reason, and because sometimes they exhibit spectroscopic variability, types as early as G0 are considered in the class of RSGs (see discussion in González-Fernández et al. 2015).

According to the latest compilation of Local Group RSGs by Levesque & Massey (2012) the most frequent spectral spectral type shifts from M2 I in the Milky Way and the LMC, to mid-K types in the SMC and to K0–1 in WLM ( $1/7$ – $1/10 Z_{\odot}$ ). The RSG-candidate SD-4, with spectral type G0–2 I, extends the spanned range of metallicity down to  $Z=1/21 Z_{\odot}$  and supports the metallicity dependence of the RSG spectral types.

#### 5 SUMMARY AND CONCLUSIONS

This paper presents the first spectroscopic census and confirmation of massive stars in SagDIG. GTC–OSIRIS optical spectroscopy has unveiled three OBA–type stars in the galaxy, and one red supergiant candidate. Pending the quantitative analysis of high-resolution optical and UV spectroscopy (e.g. Garcia et al. 2014), these could be the most iron-poor massive stars of the Local Group.

The G0–2 I spectral type of the RSG-candidate SD-4 is consistent with the reported trend of earlier RSGs spectral types in environments of lower metallicity (Levesque & Massey 2012). It extends the sequence down to  $Z=1/10$ – $1/20 Z_{\odot}$ .

The four massive stars have been found in the Eastern part of the galaxy, matching extended UV emission, and close to the highest concentrations of neutral hydrogen. Their CMD location relative to theoretical isochrones is consistent with their spectral types as long as colour excess  $E(B - V) \gtrsim 0.22$ , larger than the foreground value, is considered. This demonstrates that internal reddening in SagDIG is not negligible, and that the selection of candidate massive stars exclusively from their location at the optical CMD could dismiss a significant fraction of good candidates.

This paper opens the way to use SagDIG as a benchmark for studies of metal-poor massive stars. The most urgent follow-up is high-SNR, mid-resolution spectra of the reported stars in order to confirm their low metal content. The census of massive stars must also be completed, and this requires deep multi-object spectroscopic observations. In this respect, SagDIG is an ideal target for VLT–MUSE. By providing spectra of all the stars in the field of view, MUSE will bypass the shortcomings of reddening and target-selection biases. Observations are already planned.

#### ACKNOWLEDGMENTS

M. Garcia would like to thank F. Najarro for fruitful discussions and support from grants FIS2012-39162-C06-01, ESP2013-47809-C3-1-R and ESP2015-65597-C4-1-R. Ricardo Dorda is thanked for his library of standard stars. This research used NASA’s Astrophysics Data System, the SIMBAD database (Wenger et al. 2000), and the Aladin Sky Atlas (Bonnarel et al. 2000; Boch & Fernique 2014).

#### REFERENCES

- Asplund, M., Grevesse, N., Sauval, A. J., & Scott, P. 2009, *ARA&A*, 47, 481
- Beccari, G., Bellazzini, M., Fraternali, F., et al. 2014, *A&A*, 570, AA78, **B14**
- Boch, T., & Fernique, P. 2014, *Astronomical Data Analysis Software and Systems XXIII*, 485, 277
- Bonnarel, F., Fernique, P., Bienaymé, O., et al. 2000, *A&AS*, 143, 33
- Bouret, J.-C., Lanz, T., Hillier, D. J., et al. 2015, *MNRAS*, 449, 1545
- Bresolin, F., Urbaneja, M. A., Gieren, W., Pietrzyński, G., & Kudritzki, R.-P. 2007, *ApJ*, 671, 2028
- Camacho, I., Garcia, M., Herrero, A., & Simón-Díaz, S. 2016, *A&A*, 585, A82
- Castro, N., Herrero, A., Garcia, M., et al. 2008, *A&A*, 485, 41
- Cox, A. N. 2000, *Allen’s Astrophysical Quantities*, Springer, 2000. Edited by Arthur N. Cox. ISBN: 0387987460
- Davies, B., Origlia, L., Kudritzki, R.-P., et al. 2009, *ApJ*, 696, 2014
- Dorda, R. 2016, PhD thesis, Universidad de Alicante
- Elias, J. H., Frogel, J. A., & Humphreys, R. M. 1985, *ApJS*, 57, 91
- Filho, M. E., Sánchez Almeida, J., Muñoz-Tuñón, C., et al. 2015, *ApJ*, 802, 82
- Garcia, M., & Herrero, A. 2013, *A&A*, 551, A74
- Garcia, M., Herrero, A., Najarro, F., Lennon, D. J., & Alejandro Urbaneja, M. 2014, *ApJ*, 788, 64
- Gazak, J. Z., Kudritzki, R., Evans, C., et al. 2015, *ApJ*, 805, 182
- González-Fernández, C., Dorda, R., Negueruela, I., & Marco, A. 2015, *A&A*, 578, A3
- Greivich, J., & Putman, M. E. 2009, *ApJ*, 696, 385
- Groh, J. H., Meynet, G., Georgy, C., & Ekström, S. 2013, *A&A*, 558, A131
- Herrero, A., et al. 2010, *A&A*, 513, A70
- Hosek, M. W., Jr., et al. 2014, *ApJ*, 785, 151
- Karachentsev, I., Aparicio, A., & Makarova, L. 1999, *A&A*, 352, 363
- Kaufer, A., Venn, K. A., Tolstoy, E., Pinte, C., & Kudritzki, R.-P. 2004, *AJ*, 127, 2723
- Lee, H., Grebel, E. K., & Hodge, P. W. 2003, *A&A*, 401, 141
- Levesque, E. M., & Massey, P. 2012, *AJ*, 144, 2
- Madau, P., & Dickinson, M. 2014, *ARA&A*, 52, 415
- Marigo, P., Girardi, L., Bressan, A., et al. 2017, *ApJ*, 835, 77
- Massey, P. 1998, *Stellar astrophysics for the local group: VIII Canary Islands Winter School of Astrophysics*, 95
- McConnachie, A. W. 2012, *AJ*, 144, 4
- Momany, Y., Held, E. V., Saviane, I., et al. 2005, *A&A*, 439, 111
- Momany, Y., Clemens, M., Bedin, L. R., et al. 2014, *A&A*, 572, A42, **M14**
- Rejkuba, M., Greggio, L., Harris, W. E., Harris, G. L. H., & Peng, E. W. 2005, *ApJ*, 631, 262
- Saviane, I., Rizzi, L., Held, E. V., Bresolin, F., & Momany, Y. 2002, *A&A*, 390, 59
- Sirianni, M., Jee, M. J., Benítez, N., et al. 2005, *PASP*, 117, 1049
- Strobel, N. V., Hodge, P., & Kennicutt, R. C., Jr. 1991, *ApJ*, 383, 148
- Tang, J., Bressan, A., Slemmer, A., et al. 2016, *MNRAS*, 455, 3393
- Tramper, F., et al. 2011, *ApJ*, 741, L8
- Wenger, M., Ochsenbein, F., Egret, D., et al. 2000, *A&AS*, 143, 9
- Young, L. M., & Lo, K. Y. 1997, *ApJ*, 490, 710

This paper has been typeset from a  $\text{\TeX}/\text{\LaTeX}$  file prepared by the author.